Journal of Power Sources 271 (2014) 401–405

Contents lists available at ScienceDirect

Journal of Power Sources

journal homepage: www.elsevier.com/locate/jpowsour

Short communication

Modified pulse electrodeposition of Pt nanocatalyst as high-performance electrode for PEMFC

F. Fouda-Onana [a, *], N. Guillet [a], A.M. AlMayouf [b]

[a] Commissariat à l'Énergie Atomique et aux Énergies Alternatives, Centre de Grenoble – DRT/LITEN/DEHT/LCPEM, 17, rue des Martyrs, F 38054 Grenoble Cedex 9, France
[b] King Saud University, Chemical Engineering Dpt, College of Engineering, PO Box 800, Riyadh 11421, Saudi Arabia

HIGHLIGHTS

- We use the electrodeposition technique to prepare Pt PEMFC cathode.
- We change the electrodeposition signal to increase surface/volume ratio.
- Electrodeposited electrodes exhibit higher TOF than conventional cathode.
- Electrodeposited cathodes are close to the DOE targets à 0.9 V_{IRfree}.

ARTICLE INFO

Article history:
Received 18 March 2014
Received in revised form
24 July 2014
Accepted 7 August 2014
Available online 15 August 2014

Keywords:
Platinum
Electrodeposition
PEMFC
Catalyst utilization rate

ABSTRACT

Low platinum loading electrode was successfully deposited by a modified pulse galvanic signal in H_2PtCl_6 electrolyte using carbon black as support directly on a GDL (Gas Diffusion Layer). SEM images of the deposition were composed by rough Pt particles of 50 nm leading to specific electrochemical surface area of 53 $m^2\ g^{-1}$. In spite of large particle size and a low cathode loading of 0.12 mg cm^{-2}, the proton exchange membrane fuel cell (PEMFC) fed with humidified H_2 and O_2 at 80 °C, 1.5 absolute bar reached 0.2 mA cm_{Pt}^{-2} and 0.1 A mg^{-1} at 0.9 $V_{IR\text{-}free}$ which were twice higher than a reference membrane electrodes assembly (MEA) with a cathode loaded at 0.4 $mg_{Pt}.cm^{-2}$. Such an active cathode electrode may be ascribed to a higher utilization rate of the platinum caused by an efficient catalyst deposition by electrochemical route.

1. Introduction

Highly dispersed noble metals (platinum and platinum alloys) on high surface area carbon powders such as carbon blacks, are currently the most widely used electrocatalysts for both oxygen reduction and hydrogen oxidation in PEM fuel cell systems [1–3]. Their use in fuel cells electrodes was a breakthrough in 1990 in fuel cell performance [4,5] since high power density PEMFC was achieved reducing the platinum loading by a factor of 10. Such an improvement can be attributed to both a higher electrochemically active surface area of the carbon supported catalysts than the unsupported previously developed electrocatalyst (typical particle size about 10–20 nm) and also to the impregnation of the active catalyst layer with a soluble form of the polymer electrolyte. This allowed increasing the protonic contact between the electrolyte and the surface of the platinum catalyst within the porous carbon structure, thus permitting a more efficient use of platinum particles.

Carbon supported electrocatalyst can be prepared by several ways: chemical reduction of metal salts [6–8] chemical vapor deposition [9–11], physical deposition [12–14] or impregnation [15–17].

However, in all cases, the platinum nanoparticles are randomly dispersed in the catalytic layer and only a fraction of the noble metal is used [18,19]. Sluggish oxygen reduction reaction (ORR) kinetics requires high amount of electrochemically active platinum sites. For automotive application (hydrogen/air supply, 150 kPa), the minimum cathode platinum loading to reach an acceptable power density is about 100 $\mu g_{Pt}\ cm^{-2}$ [20], that leads toa platinum specific power density of between 1 and 2 $g_{Pt}\ kW^{-1}$.

To enhance the PEMFC performance without increasing the platinum loading, it is necessary to deposit the platinum particles

* Corresponding author.
E-mail address: frederic.fouda-onana@cea.fr (F. Fouda-Onana).

http://dx.doi.org/10.1016/j.jpowsour.2014.08.031
0378-7753/

only where it is electrochemically active. Electrodeposition, a simple process commonly used in the industry can be used to this end. The concept of Pt electrodeposition for cathode electrode has been proposed since 1990 by Vilambi [21] and pursued by many research laboratories [22–28]. However the reduction of the particle size remains a challenge. Electrodeposited Pt particles agglomerates are 200 nm large and the beneficial effect of the electrodeposition is balanced by a high loading to compensate the low surface area.

In this communication, an alternative signal to the common pulse galvanic deposition is proposed to reduce the particle size. A dead time (θ_{DT}) between two successive trains of pulses allow Pt^{4+} to diffuse up to the electrode surface and be reduced instantaneously when the galvanic current is applied. The effect of θ_{DT} during the pulsed deposition is shown from SEM images, then a comparative study of the so-made electrode labeled MEA-1 with a reference MEA-2 prepared from a commercial carbon supported platinum nanoparticles catalyst will be presented. Analyses of the polarization curves in term of mass activities and turnover frequency (TOF) show the improved activity of the electrodeposited Pt electrodes.

2. Experimental

2.1. Chemicals and solutions

A 30 mM solution of Pt precursor was prepared, with $H_2PtCl_6xH_2O$ (Sigma Aldrich) in 0.5 M H_2SO_4. 1 ml of hydrophilic ink composed by 30 mg of carbon black (acid treated Vulcan XC-72), 1.8 ml of isopropanol, 0.35 ml of 5 wt.% Nafion dispersion (D521, Dupont) and 30 μl of glycerol was vigorously sonicated before spraying on a GDL SGL-24 BC.

2.2. Instrumentation

The platinum electrodeposition was performed in a home-made three electrodes cell connected to a Versastat 3 (PAR) potentiostat with tantalum foam as counter electrodeand a silver/silver chloride (3 M AgCl solution) as reference electrode (0.197 V_{RHE}). The working electrode area was 25 cm^2.

After the Pt deposition, the sample was rinsed by immersion in deionized water.

Platinum particles shape was observed with a field emission gun scanning electron microscope (FEG-SEM) Leo 1530. Crystallite sizes were estimated by x-ray diffraction (XRD) patterns using a diffractometer (Bruker D8 Advances) using the Cu K_α radiation source ($\lambda = 1.54$ Å) in $\theta - 2\theta$ mode.

2.3. Pt electrodeposition

The Platinum deposition was carried out by pulsed galvanic deposition (PGD) using a modified signal. A PGD cycle is composed by a peak deposition current (j_{pc}) applied for θ_{on} and released for θ_{off} and repeated n_{peaks} times. The duty cycle $\theta = \theta_{on}/\theta_{on} + \theta_{off}$ falls in the range of 2–20% that fixes values of θ_{off} for a given θ_{on} value. Applying such a signal showed a constant electrode potential after 100 s of deposition. In this regard, we assumed that the interface electrode/electrolyte might be composed by a thin film of platinum and was unfavorable to promote the Pt nucleation process. By adding a rest time θ_{DT} between two PGD, we allow Pt^{4+} to diffuse to the electrode surface and to be reduced when the next current pulse is applied, thus encouraging the formation of Pt nanoparticles.

The input signal parameters were the following:

$\theta_{on} = 1$ ms, $\theta_{off} = 18$ ms, $j_{pc} = 100$ mA cm^{-2}, $n_{peaks} = 800$, $\theta_{DT} = 45$ s, Loop = 8.

The number of loops (number of times the PGD is repeated) and the others parameters are adjusted to the required coulombic charge and the smallest particle size. The Pt loading is measured with ICP-AES analyses since the hydrogen evolution reaction which is the competing reaction, does not allow the use of the faraday law to evaluate the deposited Pt.

2.4. Electrochemical characterizations

The electrochemical surface area (ECSA) of Pt is estimated from the electrode cyclic voltammogram (CV) in 0.5 M H_2SO_4 saturated with N_2 between 0.05 V and 0.3 V_{RHE} at 20 mV s^{-1}. The roughness factor (R_f) is evaluated from the following expression:

$$R_{f_{exp}} = \frac{ECSA}{S_{geo}} = \frac{Q_{Hupd}}{S_{geo} \times 0.21} \quad (1)$$

Q_{Hupd} (C) stands for the coulombic charge obtained by the integration of CV in the hydrogen desorption region. S_{geo} is the geometric surface of the electrode (25 cm^2) and the electrical charge associated with monolayer adsorption of hydrogen on polycrystalline platinum is assumed to 210 μC $cm^{-2}{}_{Pt}$.

A 5 cm^2 piece of so-prepared electrode was hot pressed with a membrane Nafion NRE 212CS and an electrode with 0.4 mg_{Pt} cm^{-2} of carbon supported Pt (Pt/C 46 wt.% Tanaka Kikinzoku Int.). This anode was prepared by coating a GDL SGL-24BC with a slurry containing a dry content of 75 wt.% of catalyst and 25 wt.% of Nafion. The MEA was then tested on PEMFC test bench at 80 °C with humidified gases: H_2 (100% RH) − O_2 (50% RH), at two different pressures: 150 and 250 kPa; $s_{H2} = 1.2$, $s_{O2} = 1.5$.

3. Results and discussion

3.1. ECSA analyses

The consequence of the rest time θ_{DT} between two PGD is shown on SEM images of Fig. 1. Pt agglomerates was reduced from 250 nm to less than 50 nm when adding the rest time. As shown on Fig. 1, Pt particles are clearly composed of agglomerated crystallites. Their typical size was determined using Scherrer law from XRD patterns shown on Fig. 2, and are in the range of 5 nm. Such a structure should increases the roughness of the particle and leads to a higher surface area.

The roughness factor (R_f) was experimentally determined using the equation (1) and was found to be 64 $cm^2{}_{Pt}$ $cm^{-2}{}_{geo}$.

If we consider this electrode as a packing of uniform spherical Pt particles of 50 nm diameter; for a platinum loading of 120 μg_{Pt} cm^{-2} and a Pt density of $\rho_{Pt} = 21$ g cm^{-3}, the roughness factor can be calculated using equation (2) and would be $R_f = 6.9$ $cm^2{}_{Pt}$ $cm^{-2}{}_{geo}$.

$$R_{f_{theo}} = \frac{3 \times \text{Loading}(mg_{Pt} \cdot cm^{-2})}{\rho_{Pt}(g \cdot cm^{-3}) \times r_{Pt}(nm)} \times 10^4 \quad (2)$$

This value is far lower than the experimentally determined one.

Interestingly, considering an electrode with a R_f of 64 for the same loading, the particle size would be about 5 nm which is in the range of the value that was found from XRD pattern.

It is possible to define a platinum utilization rate as the ratio between the practical roughness factor based on the charge for H_{upd} (Cf. eq. (1)) and the R_f value based on the Pt particle size (Cf. eq. (2)). The utilization rate for the both electrodes gave 93% and the 72% for the electrochemically deposited Pt electrode and the reference electrode respectively.

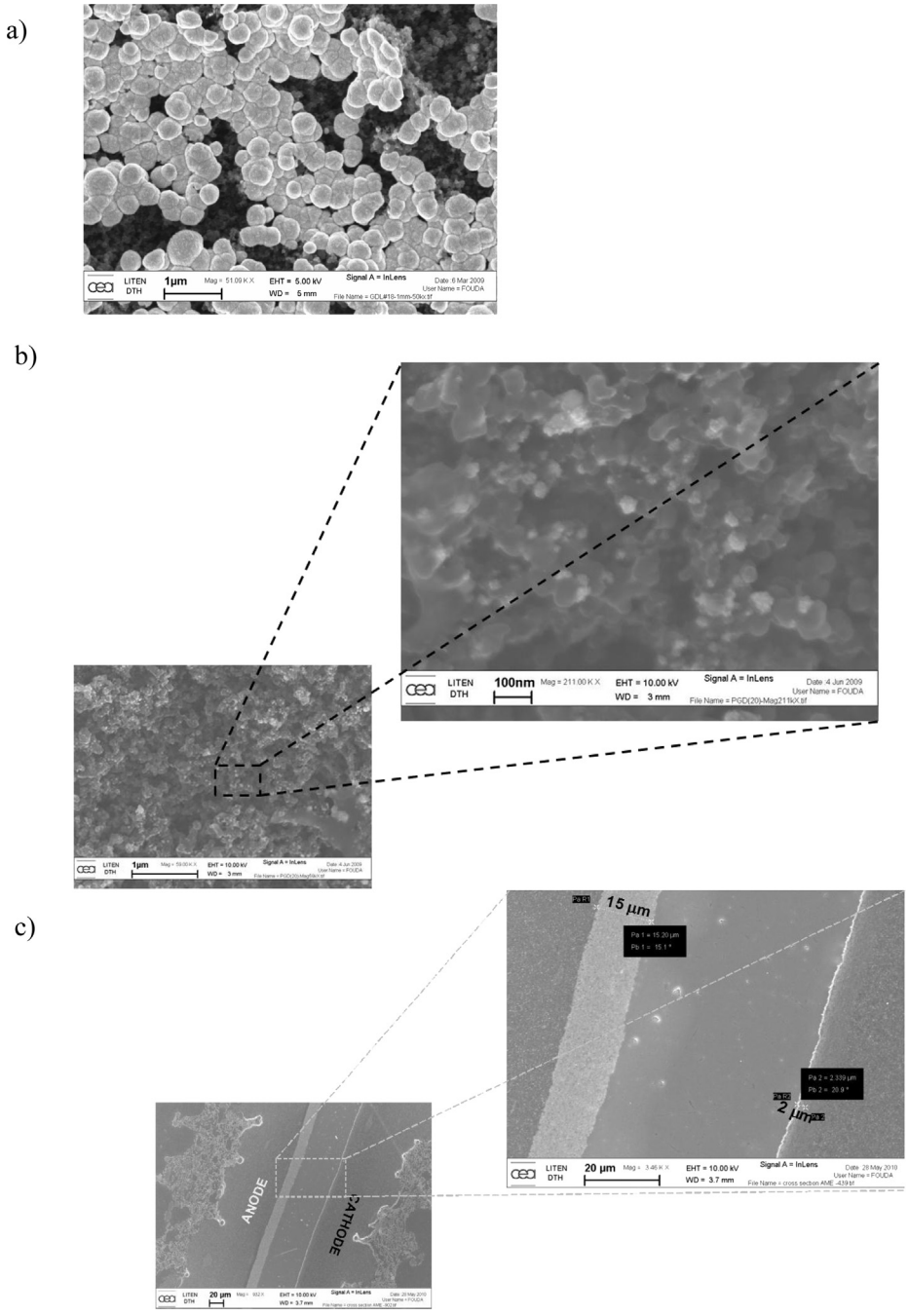

Fig. 1. SEM images of Pt electrode by electrodeposition a) Pure PGD signal deposition without rest time between deposition cycles b) modified PGD signal deposition with rets time between cycles c) cross view of the MEA comprising an electrodeposited Pt electrode (usual carbon black supported Pt nanoparticles, 15 μm thick and 450 $\mu g_{Pt}\ cm^{-2}$, on the left side; electrodeposited electrode, 2 μm thick and 120 $\mu g_{Pt}\ cm^{-2}$, on the right side).

This result points out that the higher utilization rate of the electrodeposited catalyst electrode are caused by the fact Pt catalyst are located where both conditions ionic and electrical transport are fulfilled.

3.2. MEA testing

The Pt electrodeposited electrode was used as cathode for PEMFC (5 cm^2 single cell) and will be denoted MEA-1. Fuel cell performances were compared with a reference MEA prepared with two electrodes (anode and cathode) made from 450 $\mu g_{Pt}.cm^{-2}$ carbon black supported platinum (Pt/C 46 wt.% Tanaka Kikonzoku catalyst) and denoted MEA-2. Fig. 3 presents the fuel cell output expressed in current density and mass current. As shown in Fig. 3a), in spite of a low loading and a low R_f value, MEA-1 performs as well as the reference. After normalizing the current density with the cathode platinum mass MEA-1 clearly outperforms MEA-REF (Cf. Fig. 3b)).

To eliminate any effect of the roughness or catalyst loading, the currents at 0.9 V with the ohmic drop correction (noted thereafter iR-free) were normalized with respect to the ECSA and the Pt loading and reported in Table 1. In both cases, the MEA-1 performs

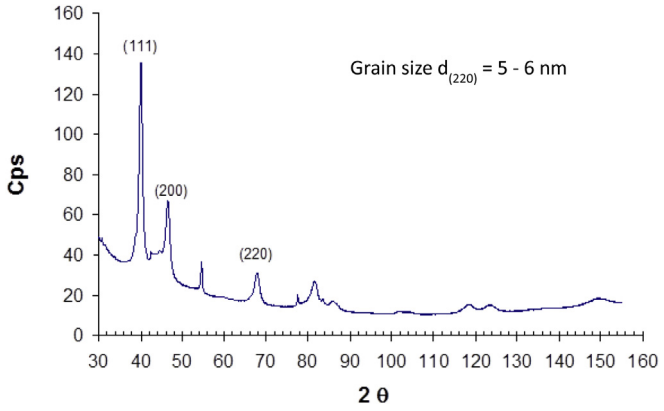

Fig. 2. X-ray diffraction pattern of the electrochemically deposited Pt.

better than MEA-2 based on commercial catalyst. Such a result may be attributed to a better utilization rate of Pt electrochemically deposited as it was amply discussed elsewhere [29–31] and confirmed by the ECSA analyses in this work. In addition the thinness of the active layer of electrodeposited cathode (only few μm, compared to 15 μm for standard electrode using Pt/C, as shown on Fig. 1c)), may reduce the oxygen transport limitations, proton resistance and oxygen concentration gradient through this layer. Consequently most of platinum deposited participate to the ORR.

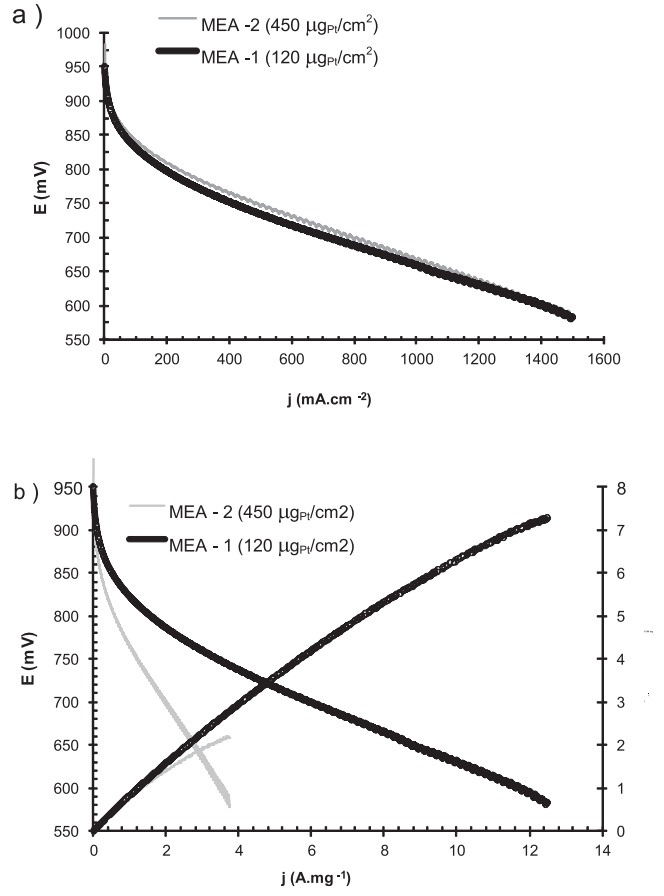

Fig. 3. Polarization curves comparison between commercial electrode and low loading electrodeposited Pt cathode electrode. Fuel cell test conditions: H_2 (100% RH) – O_2 (50% RH), 80 °C, 1.5 bar, = 1.2, = 1.5 a) Fuel cell performances b) Fuel cell mass activity performances based on cathode Pt loading.

Table 1
Comparison of the kinetic parameter two MEAs based on different platinum processing cathode.

	Cathode loading μg cm^{-2}	j @ 0,9 V mA cm^{-2}	j@ 0,9 V μA cm$_{Pt}^{-2}$	j@ 0,9 V A mg^{-1}	P @ 0,65 V W mg^{-1}
Samples					
MEA -1	120	10	156	0,08	5,5
MEA -2	450	15	65	0,03	1,8

A convenient way to assess the catalyst activity is the turnover frequency (TOF). This parameter quantifies the number of transferred electrons per active sites and per second at a given potential [19].

$$j\left(\mathrm{A\cdot cm^{-2}}\right) = \left(1.6\times10^{-19}\right)\left(C\right)\times TOF\times SD\left(\#.\mathrm{cm^{-3}}\right)\times\tau\left(\mathrm{cm}\right) \tag{3}$$

SD is the volumetric number of active sites and τ (cm) is the thickness of the active layer.

SD is evaluated from the roughness factor as follow:

$$SD\left(\#.\mathrm{cm^{-3}}\right) = \frac{R_f\left(\mathrm{cm^2_{act}}/\mathrm{cm^2_{geo}}\right)\times 0.21\left(\mathrm{mC\cdot cm^{-2}_{act}}\right)}{1.6\times10^{-19}\left(C/e^-\right)\times\tau(\mathrm{cm})}\times10^{-3} \tag{4}$$

We obtain:

$$\mathrm{TOF} = \left.\frac{j(\mathrm{A\cdot cm^{-2}})\times10^3}{R_f\times0.21\left(\mathrm{mC\cdot cm^{-2}}\right)}\right|_E \tag{5}$$

From (5), we calculated the TOF for different catalysts from works of Gasteiger et al. [19] (carbon supported catalysts) and Zhu et al. [32]. To compare the different results obtained in different operating conditions, we corrected the hydrogen permeation current, the contribution of the water saturation pressure in the total gas pressure. [19]. Assuming the reaction order of ORR to 1, we compared different fuel cell tests conditions, and we normalized the performances at 100 kPa oxygen pressure. We assumed the same ohmic drop and hydrogen permeation oxidation current for the Zhu et al. [32] and this work since the same Nafion 212 membrane was used in the both cases.

On Fig. 4, it can be noted that the values of MEA-2 and the performances of MEA from literature using the same catalyst (TEC10V50E [19]) compare quite well. The comparison of the mass activity for MEA-1 or the Zhu et al. results in which the cathode are prepared by electrodeposition performs better than commercial carbon supported catalyst (Pt/C) [19] or carbon supported Pt alloys [19].

Carbon supported Pt or Pt alloys present a TOF value about 1 e– site^{-1} s^{-1}, this value is about half of those found with the electrodeposited cathode (MEA-1 and Zhu work [32]). However, even though the mass activity is coming close to the DOE target (0,4 A mg^{-1}) when electrodeposited Pt cathode are used, the TOF values are still far below the objectives, that show lot of work is still required to develop more active catalyst for ORR.

Comparing the Zhu results with this work, their higher kinetic performances may be attributed to the different structure of the microporous layer (MPL) of the buckypaper which is considered more porous. This may reduce the O_2 transport compared with the SGL's MPL.

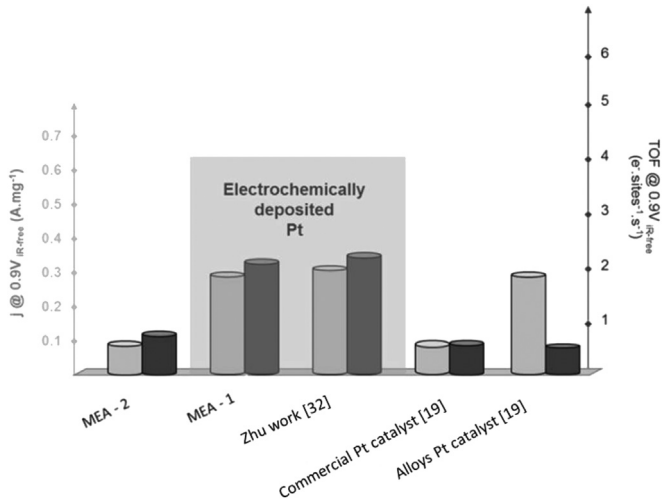

Fig. 4. Intrinsic catalytic parameters comparison between Pt electrochemically deposited and randomly deposited by chemical route. (Correction of IR drop, Hydrogen permeation and considering oxygen pressure to 1 bar assuming a reaction order of one).

4. Conclusions

Rough Pt agglomerates with typical size of 50 nm were electrochemically deposited and successfully used as cathode for PEMFC membrane – electrodes assemblies. Despite such a large particle size, the Pt utilization with the fuel cell fed with humidified H_2 and O_2 at 80 °C and 150 kPa were 0.2 g kW^{-1} at 0.65 V. Mass activity and TOF calculated at 0.9 $V_{iR\text{-}free}$ exceeded the values of the state of the art catalyst cathode. This study provides new results that confirm the higher utilization rate when the catalyst is electrochemically deposited. Even though Pt catalysts are large, the surface roughness allows obtaining high R_f value. Moreover, it is well admitted that agglomeration of 3–5 nm Pt nanoparticles may be a cause of low cathode durability. We suppose that such agglomerated electrodeposited Pt particles could mitigate the ageing of the fuel cell. Subsequent work will focus on this topic and more drastic conditions for automotive application.

Acknowledgment

Financial support for this work from King Saud University is greatly acknowledged.

References

[1] E. Antolini, Appl. Catal. B Environ. 88 (1–2) (Apr. 2009) 1–24.
[2] Fuel Cell Catalysts – Johnson Matthey Fuel Cells.
[3] Tanaka Precious Metals – Pt and Pt Ru Alloy Carbon Catalysts for PEFCs.
[4] D. Raistrick, Ian, United States Patent 4876115 electrode assembly for use in a solid polymer elecirolyte fuel cell, 1989.
[5] P. Costamagna and S. Srinivasan, Quantum jumps in the PEMFC science and technology from the 1960s to the year 2000 Part I, Fundamental scientific aspects, 102, 242–252, 2001.
[6] E. Antolini, J.R.C. Salgado, E.R. Gonzalez, J. Power Sources 160 (2) (Oct. 2006) 957–968.
[7] T. Ioroi, K. Yasuda, J. Electrochem. Soc. 152 (10) (2005) A1917.
[8] P. Kim, J.B. Joo, W. Kim, J. Kim, I.K. Song, J. Yi, J. Power Sources 160 (2) (Oct. 2006) 987–990.
[9] S. Mailley, F. Sanchette, S. Thollon, and F. Emieux, European Patent, EP 1979965 B1 Cathode pour réacteur électrochimique, réacteur électrochimique intégrant de telles cathodes et procédé de fabrication d'une telle cathode, 2009.
[10] S. Mailley, P. Capron, S. Thollon, and T. Krebs, European Patent EP 1982371B1 Procédé DLI-MOCVD pour la fabrication d'électrodes pour réacteurs électrochimiques, 2009.
[11] P. Fugier, S. Passot, C. Anglade, L. Guetaz, N. Guillet, E. De Vito, S. Mailley, A. a . Franco, J. Electrochem. Soc. 157 (6) (2010) B943.
[12] D. Fofana, S.K. Natarajan, P. Bénard, J. Hamelin, ISRN Electrochem. 2013 (2013) 1–6.
[13] M. Cavarroc, a. Ennadjaoui, M. Mougenot, P. Brault, R. Escalier, Y. Tessier, J. Durand, S. Roualdès, T. Sauvage, C. Coutanceau, Electrochem. Commun. 11 (4) (Apr. 2009) 859–861.
[14] a Caillard, C. Charles, R. Boswell, P. Brault, J. Phys. D Appl. Phys. 41 (18) (Sep. 2008) 185307.
[15] X. Hao, S. Barnes, J.R. Regalbuto, J. Catal. 279 (1) (Apr. 2011) 48–65.
[16] N. Job, M. Chatenet, S. Berthon-Fabry, S. Hermans, F. Maillard, J. Power Sources 240 (Oct. 2013) 294–305.
[17] N. Job, S. Lambert, M. Chatenet, C.J. Gommes, F. Maillard, S. Berthon-Fabry, J.R. Regalbuto, J.-P. Pirard, Catal. Today 150 (1–2) (Feb. 2010) 119–127.
[18] K. Shinozaki, H. Yamada, Y. Morimoto, J. Electrochem. Soc. 158 (5) (2011) B467.
[19] H. a. Gasteiger, S.S. Kocha, B. Sompalli, F.T. Wagner, Appl. Catal. B Environ. 56 (1–2) (Mar. 2005) 9–35.
[20] E. Billy, F. Maillard, a. Morin, L. Guetaz, F. Emieux, C. Thurier, P. Doppelt, S. Donet, S. . Mailley, J. Power Sources 195 (9) (May 2010) 2737–2746.
[21] E.B. Anderson and J. Earl, United States Patent [19], 1992.
[22] a. J. Martín, a. M. Chaparro, B. . Gallardo, M. a. Folgado, L. Daza, J. Power Sources 192 (1) (Jul. 2009) 14–20.
[23] K. Saminathan, V. Kamavaram, V. Veedu, a. M. . Kannan, Int. J. Hydrogen Energy 34 (9) (May 2009) 3838–3844.
[24] M.S. Chandrasekar, M. Pushpavanam, Electrochim. Acta 53 (8) (Mar. 2008) 3313–3322.
[25] S.M. Ayyadurai, Y.-S. Choi, P. Ganesan, S.P. Kumaraguru, B.N. Popov, J. Electrochem. Soc. 154 (10) (2007) B1063.
[26] K.H. Choi, H.S. Kim, T.H. Lee, J. Power Sources 75 (2) (Oct. 1998) 230–235.
[27] S.D. Thompson, L.R. Jordan, M. Forsyth, Electrochim. Acta 46 (10–11) (Mar. 2001) 1657–1663.
[28] C. Paoletti, A. Cemmi, L. Giorgi, R. Giorgi, L. Pilloni, E. Serra, M. Pasquali, J. Power Sources 183 (1) (Aug. 2008) 84–91.
[29] Z.D. Wei, S.G. Chen, Y. Liu, C.X. Sun, Z.G. Shao, P.K. Shen, J. Phys. Chem. C 111 (42) (Oct. 2007) 15456–15463.
[30] Y. Ra, J. Lee, I. Kim, S. Bong, H. Kim, J. Power Sources 187 (2) (Feb. 2009) 363–370.
[31] S. Litster, G. McLean, J. Power Sources 130 (1–2) (May 2004) 61–76.
[32] W. Zhu, D. Ku, J.P. Zheng, Z. Liang, B. Wang, C. Zhang, S. Walsh, G. Au, E.J. Plichta, Electrochim. Acta 55 (7) (Feb. 2010) 2555–2560.